Analysis and Synthesis of Stable Grasp by Multi-Fingered Robot Hand with Compliance Control

Akira Nakashima, Yuta Yoshimastsu and Yoshikazu Hayakawa

***Abstract*— In this paper, we deal with an analysis and a synthesis of stable grasp by a multi-fingered robot hand with compliance control. The stability of a grasped object by the fingers with linear elastic stiffness is firstly analyzed. A sufficient condition with the gravity effect is driven with respect to the contact points, the elastic coefficients and the mass of the grasped object. A compliance controller with a disturbance observer using force sensors secondly is proposed. The stability of the controller is proved by the Lyapunov stability theorem. The performance of the controller is verified in experiments. Furthermore, it is verified that the grasp by the compliance controller is stable with the sufficient condition.**

I. Introduction

Many researchers have tried to introduce robots into human's daily environments. Since the robots are aimed to do various tasks instead of human, multi-fingered robot hands are effective as end-effectors. Multi-fingered robot hands have capability to grasp variously-shaped objects because the hands can grasp with multi contacts and can control grasping force via multi joint inputs.

There are two major methodologies to deal with the grasp stability. The first one is the optimization of the contact forces with the *Force-Closure* [1]. Kerr et al. [2] considered an optimization method of the contact forces to maximize the distances of the forces from the boundaries derived by the frictional condition and the joint torque limitation. Nakamura et al. [3] derived minimum forces to satisfy the equilibrium of the forces and the frictional condition so as to prevent the break of the grasped object. As examples of other kinds of research, there are the force decomposition to manipulating and grasping forces [4] and a force determination with the Force- and Form-Closures [5].

In the second one, the stability is discussed based on the *stiffness-effect* [6], which is the resultant force and moment due to unbalanced contact forces with the linear elastic stiffness when the grasped object is perturbed from its equilibrium point. Hanafusa et al. [7] considered the grasp by fingers, each of which is assumed to be one degree of freedom (DOF) spring. They derived that the grasp was stable when the elastic energy due to the fingers was minimum around the equilibrium of the forces. This means that the stiffness effect by the contact forces is the *restoring force* against the perturbation. Kaneko et al. [8] considered the grasp in the case of the fingers with two DOF springs and showed that the spring corresponding to friction forces effected on the grasp stability. Yamada et al. [9] considered the effect of the rolling contact on the stability. In these studies, it is assumed that the mass of the object is not considered because of the complexity of the analysis. However, it is important to consider the *gravity effect* which destabilizes the grasp.

The elastic stiffness of the fingers in the previous studies is synthesized by compliance control methods for the fingers, where it is necessary to compensate the *degeneration factors* such as model uncertainties, gravity term, joint elasticity and joint friction. Ott et al. [10] estimated the joint angles with the joint elasticity and realized the approximated compliance with the gravity compensation by its iterative calculation. Doulgeri and Arimoto [11] proposed an adaptive compliance control for the kinematic uncertainties. Chen et al. [12] identified the joint friction as the sum of the static and dynamic friction with the two relay circuits.

While these studies compensate only the specified factors, the *disturbance observer* [13] treats all the factors except for the nominal inertia and the control input as the disturbance. The disturbance observer is applied for the servo control [14], [15], the force control [16], [17] and the compliance control [18], [19] because of its simplicity and high control performance. However, there is few studies of the stability analysis due to the complexity of the disturbance signal, which includes the *various* types of the degeneration factors. Kaneko et al. [20] discussed the effect of the inertia variation based on the root locus *numerically*. The variation of the torque coefficient was considered in [21]. Since these analyses were carried out based on the root locus, the control parameters must be iteratively tuned by *graphical and intuitive* method. Furthermore, it is impossible to confirm that the whole system with the determined parameters is stable *before* applying the controller to the system.

In this paper, we deal with an analysis and a synthesis of stable grasp by a multi-fingered robot hand with compliance control. The stability of a grasped object by the fingers with linear elastic stiffness is firstly analyzed. A sufficient condition with the gravity effect is driven with respect to the contact points, the elastic coefficients and the mass of the grasped object. A compliance controller with a disturbance observer using force sensors secondly is secondly proposed. The stability of the controller is proved by the Lyapunov stability theorem with a sufficient condition. Since this condition is composed of analytical equations, it is possible to design control parameters to guarantee the stability. The performance of the controller is verified in experiments.

Authors are with Mechanical Science and Engineering, Graduate School of Engineering, Nagoya University, Furo-cho, Chikusa-ku, Nagoya, Japan akira@haya.nuem.nagoya-u.ac.jp, and Y. Hayakawa is also with RIKEN-TRI Collaboration Center, RIKEN, 2271-103, Anagahora, Shimoshidami, Moriyama-ku, Nagoya, Japan.

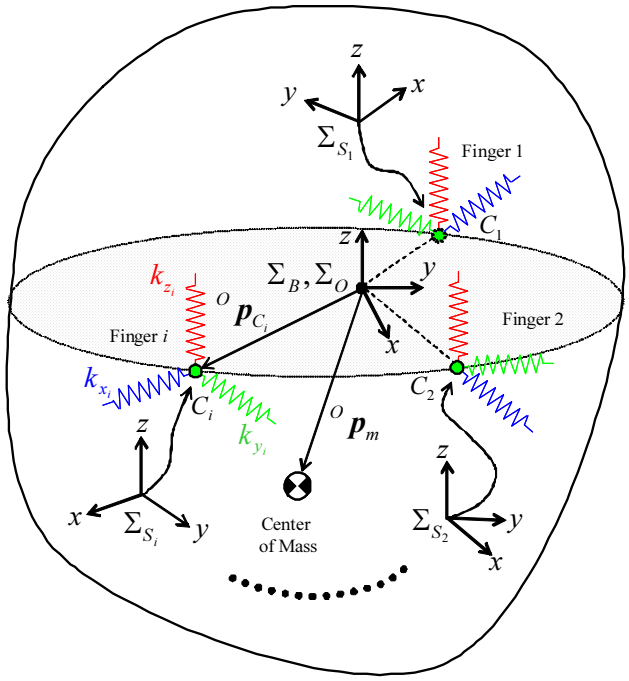

Fig. 1. An object grasped by virtual spring fingers.

Furthermore, it is verified that the grasp by the compliance controller is stable with the sufficient condition.

II. Stability Analysis of Grasp

A. Problem setting

Consider an object grasped by ith virtual linear spring at ith contact points C_i ($i = 1, \cdots, n$) as shown in Fig. 1. Σ_B is the base frame and Σ_O is the object frame fixed to the object. Σ_O is represented by the position vector $\boldsymbol{p}_O \in \mathbb{R}^3$ and the rotation matrix $\boldsymbol{R}_O \in \mathbb{R}^{3\times3}$ of Σ_O from Σ_B. Σ_B and Σ_O are assumed to coincide to each other at the initial state. The contact C_i and the center of mass of the object are represented by ${}^O\boldsymbol{p}_{C_i} \in \mathbb{R}^3$ and ${}^O\boldsymbol{p}_m \in \mathbb{R}^3$ expressed in Σ_O. In the latter, vectors without left superscripts are expressed in Σ_B. The spring frame Σ_{S_i} is fixed to the space with the origin which coincides to C_i at the initial state for the representation of the spring displacements. $\boldsymbol{p}_{S_i} \in \mathbb{R}^3$ and $\boldsymbol{R}_{S_i} \in \mathbb{R}^{3\times3}$ are the position and orientation of Σ_{S_i}. The spring displacements $\boldsymbol{\delta}_i := [\delta_{x_i}\ \delta_{y_i}\ \delta_{z_i}]^{\mathrm{T}} \in \mathbb{R}^3$ are defined as the coordinates in Σ_{S_i}. $\delta_{*i} > 0$ and $\delta_{*i} < 0$ express the compression and extension from the natural thinning. Note that $*$ denotes x, y or z. The stiffness coefficients are denoted by $\boldsymbol{K}_i :=$ block diag$(k_{x_i}, k_{y_i}, k_{z_i}) \in \mathbb{R}^{3\times3}$.

We make the following assumptions:

Assumption 1: The x- and y-axes of the spring frame Σ_{S_i} are in the same plane and the elongations of all the x-axes cross at one point. Σ_O is fixed to this point. The x- and y-axes of Σ_O and Σ_{S_i} are in the same plane.

Assumption 2: The contact forces produced by the springs and the gravity force are balanced at the initial state. The initial of the spring displacements are $\boldsymbol{\delta}_{0_i} := [\delta_{0x_i}\ 0\ -\delta_{0z_i}]^{\mathrm{T}}$ and $\delta_{0x_i},\ \delta_{0z_i} > 0$.

Assumption 3: The contact types are the fixed contact. Therefore, the contact C_i is not changed with respect to Σ_O.

From Assumptions 2, 1 and 3, the following equations hold:

$$\textstyle\sum_{i=1}^n \boldsymbol{f}_i^0 + m\boldsymbol{g} = \boldsymbol{0} \tag{1}$$

$$\textstyle\sum_{i=1}^n \boldsymbol{p}_{C_i}^0 \times \boldsymbol{f}_i^0 + \boldsymbol{p}_m^0 \times m\boldsymbol{g} = \boldsymbol{0}, \tag{2}$$

where

$$\boldsymbol{f}_i^0 := -\boldsymbol{R}_{S_i}\boldsymbol{K}_i\boldsymbol{\delta}_{0_i}. \tag{3}$$

(1) and (2) denote the equilibrium of force and moment. $\boldsymbol{f}_i^0 \in \mathbb{R}^3$ is the initial force, m is the mass of the object, $\boldsymbol{g} := [0\ 0\ -g]^{\mathrm{T}} \in \mathbb{R}^3$, $g = 9.8$ [m/s^2] is the gravity vector. $\boldsymbol{p}_{C_i}^0$ and $\boldsymbol{p}_m^0 \in \mathbb{R}^3$ are the initial contact point and the position of the center of mass given by

$$\begin{aligned}
&\boldsymbol{p}_{C_i}^0 = \boldsymbol{p}_{S_i},\ \boldsymbol{p}_m^0 = {}^O\boldsymbol{p}_m \\
&\boldsymbol{p}_{S_i} := {}^O\boldsymbol{p}_{C_i},\ \boldsymbol{R}_{S_i} := \begin{bmatrix} C_{\alpha_i} & -S_{\alpha_i} & 0 \\ S_{\alpha_i} & C_{\alpha_i} & 0 \\ 0 & 0 & 1 \end{bmatrix} \\
&{}^O\boldsymbol{p}_{C_i} := [r_iC_{\alpha_i}\ r_iS_{\alpha_i}\ 0]^{\mathrm{T}} \\
&{}^O\boldsymbol{p}_m := [r_mS_{\beta_m}C_{\alpha_m}\ r_mS_{\beta_m}S_{\alpha_m}\ r_mC_{\beta_m}]^{\mathrm{T}}.
\end{aligned} \tag{4}$$

From Assumption 3, note that $\boldsymbol{p}_{S_i}$ and ${}^O\boldsymbol{p}_m$ are constants. r_*, α_* and β_* are the polar coordinates, where α_* and β_* are the angles from the x- and z-axes and $*$ denotes i or m. For simplicity, the abbreviations $C_{\alpha_i} := \cos\alpha_i$ and $S_{\alpha_i} := \sin\alpha_i$ are used in the latter.

For the grasp mentioned here, we define the following stability:

Definition 1: When the object is perturbed from the equilibrium with any small displacement $\boldsymbol{r} \in \mathbb{R}^6$, the grasp is stable if the following relationship holds:

$$\boldsymbol{r}^{\mathrm{T}}\boldsymbol{F}_r < 0, \tag{5}$$

where $\boldsymbol{F}_r \in \mathbb{R}^6$ is the stiffness effect by the springs. Then, $\boldsymbol{F}_r$ is called as the *restoring force*.

Definition 1 is equivalent to that the potential energy of the grasp is locally minimum at the equilibrium [7].

B. A sufficient condition of the stability

The perturbation $\boldsymbol{r}$ is expressed by the position $\boldsymbol{p}_O$ and the roll-pitch-yaw orientation $\boldsymbol{\phi}_O$ of $\boldsymbol{R}_O$ as $\boldsymbol{r} := [\ \boldsymbol{p}_O^{\mathrm{T}}\ \ \boldsymbol{\phi}_O^{\mathrm{T}}\ ]^{\mathrm{T}} \in \mathbb{R}^6$. The stiffness effect $\boldsymbol{F}_r$ is derived as [7]

$$\boldsymbol{F}_r = -\boldsymbol{K}_r\boldsymbol{r}, \tag{6}$$

$$\boldsymbol{K}_r = \frac{\partial}{\partial\boldsymbol{r}}\left(\frac{\partial U}{\partial\boldsymbol{r}}\right)^{\mathrm{T}} =: \begin{bmatrix} \boldsymbol{K}_r^{pp} & \boldsymbol{K}_r^{p\phi} \\ \boldsymbol{K}_r^{p\phi} & \boldsymbol{K}_r^{\phi\phi} \end{bmatrix}, \tag{7}$$

where $U(\boldsymbol{r})$ is the potential energy of the grasp given by

$$U(\boldsymbol{r}) = \frac{1}{2}\textstyle\sum_{i=1}^n \boldsymbol{\delta}_i(\boldsymbol{r})^{\mathrm{T}}\boldsymbol{K}_i\boldsymbol{\delta}_i(\boldsymbol{r}) + \boldsymbol{p}_m(\boldsymbol{r})^{\mathrm{T}}m\boldsymbol{g}, \tag{8}$$

$$\begin{aligned}
\boldsymbol{\delta}_i(\boldsymbol{r}) &= \boldsymbol{R}_{S_i}^{-1}\{(\boldsymbol{R}_O(\boldsymbol{\phi}_O) - \boldsymbol{I}_3){}^O\boldsymbol{p}_{C_i} + \boldsymbol{p}_O\} + \boldsymbol{\delta}_{0_i} \\
\boldsymbol{p}_m(\boldsymbol{r}) &= \boldsymbol{R}_O(\boldsymbol{\phi}_O){}^O\boldsymbol{p}_m + \boldsymbol{p}_O.
\end{aligned} \tag{9}$$

$\boldsymbol{K}_r^{pp}$ represents the stiffness effect from the position to the translational force and is always positive definite [8]. $\boldsymbol{K}_r^{p\phi}$ represents the coupling between the position and orientation, which can be calculated as $\boldsymbol{K}_r^{p\phi} = \boldsymbol{0}_{3\times 3}$ by Assumption 1 and the following assumption:

$$\begin{aligned} &\textstyle\sum_{i=1}^n k_{y_i} r_i C_{\alpha_i} = 0, \quad \sum_{i=1}^n k_{y_i} r_i S_{\alpha_i} = 0 \\ &\textstyle\sum_{i=1}^n k_{z_i} r_i C_{\alpha_i} = 0, \quad \sum_{i=1}^n k_{z_i} r_i S_{\alpha_i} = 0. \end{aligned} \tag{10}$$

From (10), $\boldsymbol{K}_r$ results in

$$\boldsymbol{K}_r = \begin{bmatrix} \boldsymbol{K}_r^{pp} & \boldsymbol{0}_{3\times 3} \\ \boldsymbol{0}_{3\times 3} & \boldsymbol{K}_r^{\phi\phi} \end{bmatrix}. \tag{11}$$

Defection 1 and (6) lead to the stability condition of $\boldsymbol{K}_r$:

$$\boldsymbol{r}^{\mathrm{T}} \boldsymbol{K}_r \boldsymbol{r} > 0 \;\Leftrightarrow\; \boldsymbol{K}_r \succ 0 \tag{12}$$

From (12), (11) and $\boldsymbol{K}_r^{pp} \succ 0$, the grasp is stable when the following holds:

$$\boldsymbol{K}_r^{\phi\phi} := \begin{bmatrix} k_{11} & k_{12} & k_{13} \\ k_{12} & k_{22} & k_{23} \\ k_{13} & k_{23} & k_{33} \end{bmatrix} \succ 0, \tag{13}$$

where

$$\begin{aligned} k_{11} &= \textstyle\sum_{i=1}^n r_i S_{\alpha_i}^2 (k_{z_i} r_i - k_{x_i} \delta_{0x_i}) - r_m C_{\beta_m} mg \\ k_{22} &= \textstyle\sum_{i=1}^n r_i C_{\alpha_i}^2 (k_{z_i} r_i - k_{x_i} \delta_{0x_i}) - r_m C_{\beta_m} mg \\ k_{33} &= \textstyle\sum_{i=1}^n r_i (k_{y_i} r_i - k_{x_i} \delta_{0x_i}) \\ k_{12} &= \textstyle\sum_{i=1}^n -r_i C_{\alpha_i} S_{\alpha_i} (k_{z_i} r_i - k_{x_i} \delta_{0x_i}) \\ k_{13} &= r_m S_{\beta_m} C_{\alpha_m} mg, \;\; k_{23} = r_m S_{\beta_m} S_{\alpha_m} mg. \end{aligned} \tag{14}$$

A sufficient condition of (13) is given by the following theorem:

Theorem 1: Suppose (10) and

$$k_{z_i} r_i - k_{x_i} \delta_{0x_i} > 0 \tag{15}$$

$$k_{y_i} r_i - k_{x_i} \delta_{0x_i} > 0 \tag{16}$$

$$C_{\beta_m} < \tfrac{k_{33}}{2 r_m mg} - \sqrt{\left(\tfrac{k_{33}}{2 r_m mg}\right)^2 + 1}. \tag{17}$$

Then, $\boldsymbol{K}_r^{\phi\phi}$ is positive definite.

Proof: For simplicity, from (15) and (16), $\boldsymbol{a}$, $\boldsymbol{b}$ and $\boldsymbol{c} \in \mathbb{R}^n$ and M are defined as

$$\begin{aligned} a_i &:= S_{\alpha_i} \sqrt{r_i (k_{z_i} r_i - k_{x_i} \delta_{0x_i})} \\ b_i &:= C_{\alpha_i} \sqrt{r_i (k_{z_i} r_i - k_{x_i} \delta_{0x_i})} \\ c_i &:= \sqrt{r_i (k_{y_i} r_i - k_{x_i} \delta_{0x_i})}, \\ M &:= r_m mg. \end{aligned} \tag{18}$$

Then, $\boldsymbol{K}_r^{\phi\phi}$ is decomposed as

$$\boldsymbol{K}_r^{\phi\phi} = \boldsymbol{K}_s^{\phi} + \boldsymbol{K}_m^{\phi\phi}, \tag{19}$$

where

$$\boldsymbol{K}_s^{\phi\phi} = \begin{bmatrix} \boldsymbol{a}^{\mathrm{T}}\boldsymbol{a} & -\boldsymbol{a}^{\mathrm{T}}\boldsymbol{b} & 0 \\ -\boldsymbol{a}^{\mathrm{T}}\boldsymbol{b} & \boldsymbol{b}^{\mathrm{T}}\boldsymbol{b} & 0 \\ 0 & 0 & 0 \end{bmatrix} \tag{20}$$

$$\boldsymbol{K}_s^{\phi\phi} = \begin{bmatrix} -MC_{\beta_m} & 0 & MS_{\beta_m} C_{\alpha_m} \\ 0 & -MC_{\beta_m} & MS_{\beta_m} S_{\alpha_m} \\ MS_{\beta_m} C_{\alpha_m} & MS_{\beta_m} S_{\alpha_m} & \boldsymbol{c}^{\mathrm{T}}\boldsymbol{c} \end{bmatrix}. \tag{21}$$

Theorem 1 will be proved by decomposing the stiffness matrix $\boldsymbol{K}_r^{\phi\phi}$ to $\boldsymbol{K}_s^{\phi\phi}$ and $\boldsymbol{K}_m^{\phi\phi}$ as in (19), which are the stiffness ones due to (a_i, b_i) and (C_{β_m}, c_i) respectively. $\boldsymbol{K}_s^{\phi\phi}$ is positive semi definite because $\boldsymbol{K}_s^{\phi\phi}$ is rewritten as

$$\boldsymbol{K}_s^{\phi\phi} = \begin{bmatrix} \boldsymbol{a}^{\mathrm{T}} \\ -\boldsymbol{b}^{\mathrm{T}} \\ \boldsymbol{0}_{1\times n} \end{bmatrix} \begin{bmatrix} \boldsymbol{a}^{\mathrm{T}} \\ -\boldsymbol{b}^{\mathrm{T}} \\ \boldsymbol{0}_{1\times n} \end{bmatrix}^{\mathrm{T}}. \tag{22}$$

Therefore, it is sufficient to prove $\boldsymbol{K}_m^{\phi\phi} \succ 0$.

The necessary and sufficient condition for $\boldsymbol{K}_m^{\phi\phi} \succ 0$ is that all the principal minors $\det \boldsymbol{K}_{m_j}^{\phi\phi}$ $(j = 1, 2, 3)$ are positive. It is evident that $\det \boldsymbol{K}_{m_j}^{\phi\phi}$ $(j = 1, 2)$ are positive because C_{β_m} is negative from (17). $\det \boldsymbol{K}_{m_3}^{\phi\phi}$ is calculated as

$$\begin{aligned} \det \boldsymbol{K}_{r_3}^{\phi\phi} &= -M^3 C_{\beta_m} \left(C_{\beta_m}^2 - \frac{\boldsymbol{c}^{\mathrm{T}}\boldsymbol{c}}{M} C_{\beta_m} - 1 \right) \\ &= -M^3 C_{\beta_m} (C_{\beta_m} + d)(C_{\beta_m} - d), \end{aligned} \tag{23}$$

where

$$d := \frac{\boldsymbol{c}^{\mathrm{T}}\boldsymbol{c}}{2M} - \sqrt{\left(\frac{\boldsymbol{c}^{\mathrm{T}}\boldsymbol{c}}{2M}\right)^2 + 1}.$$

Therefore, $\det \boldsymbol{K}_{r_3}^{\phi\phi}$ is positive when

$$C_{\beta_m} < d \tag{24}$$

$$d > -1. \tag{25}$$

The first condition (24) is satisfied from (17) and (18) as illustrated in Fig. 2 (a). The second condition (25) is necessary for C_{β_m} to satisfy the first condition because of $C_{\beta_m} \geq -1$. d is rewritten as

$$d(e) = e - \sqrt{e^2 + 1} < 0, \;\; e := \frac{\boldsymbol{c}^{\mathrm{T}}\boldsymbol{c}}{2M} > 0. \tag{26}$$

It is proved that $d(e) > -1$ for any $e > 0$ because

$$\frac{d}{de} d(e) = \frac{\sqrt{e^2+1} - e}{\sqrt{e^2+1}} > 0, \;\; \lim_{e \to 0} d(e) = -1.$$

(25) is illustrated in Fig. 2 (b).

∎

Remark 1: Let us consider the physical interpretation of the sufficient conditions of the grasp stability. (a_i, b_i) represents the relation between the moment and orientation in the (x, y)-plane. Therefore, (15) means that the each finger can produce the restoring moment about any axis in the

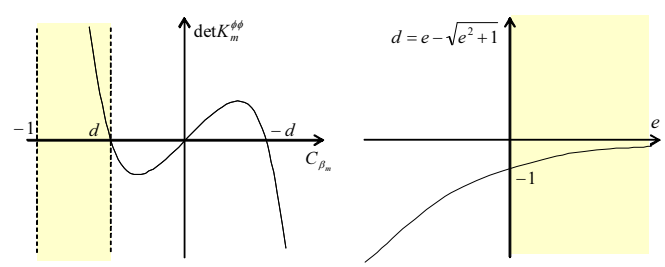

(a) The third principle minor $\det K_m^{\phi\phi}$ (b) The upper bound of C_{β_m}

Fig. 2. The determinant $\det K_{m_3}^{\phi\phi}$ and the upper bound of C_{β_m}.

(x, y)-plane by itself because $\boldsymbol{K}_s^{\phi\phi}$ is positive semi definite as in (22). On the other hand, c_i means the relation between the moment and orientation about the z-axis. C_{β_m} determines which the center of mass is above or below the contact points. Therefore, (16) means that the each finger can produce the restoring moment about the z-axis by itself and (17) means that the position of the center of mass is lower from the contact points. The upper bound $d(e)$ of C_{β_m} converges to 0 by increasing $e = \boldsymbol{c}^{\mathrm{T}}\boldsymbol{c}/(2M)$, i.e., $\boldsymbol{c}^{\mathrm{T}}\boldsymbol{c} \gg 2M$. For example, it is possible from (18) to reduce the unstable effect of the gravity by making the stable effect of c_i about the z-axis with the large stiffness coefficient k_{y_i}.

III. Synthesis of Compliance Control

A. Controller with a disturbance observer

Consider the situation of Fig. 3 where a finger with three joints is pushing the wall. Σ_P is the reference frame fixed to the base of the finger. $\boldsymbol{q} \in \mathbb{R}^3$ denotes the joint angles and $\boldsymbol{f}_{ext} \in \mathbb{R}^3$ is the external force to the finger from the wall. The subscript i is omitted for writing simplicity. The equation of motion of the finger is given by

$$\boldsymbol{M}(\boldsymbol{q})\ddot{\boldsymbol{q}} + \boldsymbol{C}(\boldsymbol{q}, \dot{\boldsymbol{q}})\dot{\boldsymbol{q}} + \boldsymbol{g}(\boldsymbol{q}) = \boldsymbol{\tau} + \boldsymbol{J}(\boldsymbol{q})^{\mathrm{T}}\boldsymbol{f}_{ext} + \boldsymbol{\tau}_f, \quad (27)$$

where $\boldsymbol{M} \in \mathbb{R}^{3\times3}$ is the inertia matrix, $\boldsymbol{C} \in \mathbb{R}^{3\times3}$ is the coriolis matrix, $\boldsymbol{g} \in \mathbb{R}^3$ is the gravity term, $\boldsymbol{\tau} \in \mathbb{R}^3$ is the input torque and $\boldsymbol{\tau}_f \in \mathbb{R}^3$ is the viscous and static friction. $\boldsymbol{J} \in \mathbb{R}^{3\times3}$ is the jacobian defined by

$$\dot{\boldsymbol{x}} = \boldsymbol{J}(\boldsymbol{q})\dot{\boldsymbol{q}}, \quad (28)$$

where $\boldsymbol{x} \in \mathbb{R}^3$ is the position of the finger expressed in Σ_P. (27) is transformed into the form in the work space via (28) as

$$\boldsymbol{M}_x\ddot{\boldsymbol{x}} + \boldsymbol{C}_x\dot{\boldsymbol{x}} + \boldsymbol{J}^{-\mathrm{T}}\boldsymbol{g} = \boldsymbol{J}^{-\mathrm{T}}\boldsymbol{\tau} + \boldsymbol{f}_{ext} + \boldsymbol{J}^{-\mathrm{T}}\boldsymbol{\tau}_f, \quad (29)$$

where

$$\boldsymbol{M}_x(\boldsymbol{q}) := \boldsymbol{J}^{-\mathrm{T}}\boldsymbol{M}(\boldsymbol{q})\boldsymbol{J}^{-1}$$
$$\boldsymbol{C}_x(\boldsymbol{q}, \dot{\boldsymbol{q}}) := \boldsymbol{J}^{-\mathrm{T}}\{\boldsymbol{C}(\dot{\boldsymbol{q}}, \boldsymbol{q}) - \boldsymbol{M}(\boldsymbol{q})\boldsymbol{J}^{-1}\dot{\boldsymbol{J}}\}\boldsymbol{J}^{-1}.$$

The objective of the compliance control is to achieve the following relationship via $\boldsymbol{\tau}$:

$$\boldsymbol{K}(\boldsymbol{x} - \boldsymbol{x}_{ref}) = \boldsymbol{f}_{ext}, \ \boldsymbol{K} \succ 0, \quad (30)$$

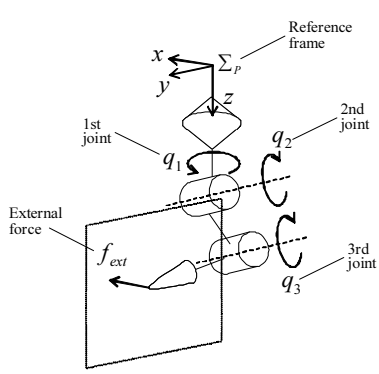

Fig. 3. A finger with 3 degrees of freedom pushing a wall.

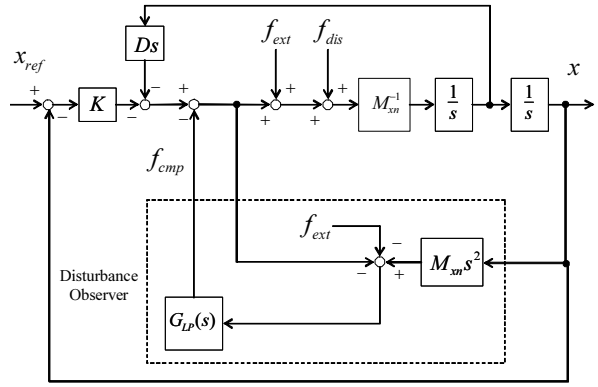

Fig. 4. The block diagram of the whole system with the disturbance observer.

where $\boldsymbol{K} \in \mathbb{R}^{3\times3}$ is the desired stiffness matrix and $\boldsymbol{x}_{ref} \in \mathbb{R}^3$ is the *constant* equilibrium position. However, it is necessary to consider dynamics in addition to (30) to enhance the stability. Therefore, the control objective is modified as

$$\boldsymbol{M}_{xn}\ddot{\boldsymbol{x}} + \boldsymbol{D}\dot{\boldsymbol{x}} + \boldsymbol{K}(\boldsymbol{x} - \boldsymbol{x}_{ref}) = \boldsymbol{f}_{ext}, \quad (31)$$

where

$$\boldsymbol{M}_{xn} := \boldsymbol{J}(\boldsymbol{q}_{ref})^{-\mathrm{T}}\boldsymbol{M}(\boldsymbol{q}_{ref})\boldsymbol{J}(\boldsymbol{q}_{ref})^{-1}, \ \boldsymbol{D} \succ 0.$$

$\boldsymbol{q}_{ref} \in \mathbb{R}^3$ corresponds to $\boldsymbol{x}_{ref}$, $\boldsymbol{M}_{xn} \in \mathbb{R}^{3\times3}$ is the nominal inertia matrix of $\boldsymbol{M}_x$ and $\boldsymbol{D} \in \mathbb{R}^{3\times3}$ is the desired viscous matrix. Note that $\boldsymbol{K}$, $\boldsymbol{M}_{xn}$ and $\boldsymbol{D}$ are positive definite.

The external force $\boldsymbol{f}_{ext}$, the joint angle and its velocity $(\boldsymbol{q}, \dot{\boldsymbol{q}})$ are available for the controller. $\boldsymbol{f}_{ext}$ and $(\boldsymbol{q}, \dot{\boldsymbol{q}})$ are measured by a force sensor and encoders. We consider the control input given by

$$\boldsymbol{\tau} = -\boldsymbol{J}^{\mathrm{T}}\{\boldsymbol{K}(\boldsymbol{x} - \boldsymbol{x}_{ref}) + \boldsymbol{D}\dot{\boldsymbol{x}} + \boldsymbol{f}_{cmp}\} + \boldsymbol{g}, \quad (32)$$

where $\boldsymbol{f}_{cmp} \in \mathbb{R}^3$ is the compensator for disturbance. Substituting (32) into (29) yields

$$\boldsymbol{M}_{xn}\ddot{\boldsymbol{x}} + \boldsymbol{D}\dot{\boldsymbol{x}} + \boldsymbol{K}(\boldsymbol{x} - \boldsymbol{x}_{ref}) = \boldsymbol{f}_{ext} + \boldsymbol{f}_{dis} - \boldsymbol{f}_{cmp}, \quad (33)$$

where

$$\boldsymbol{f}_{dis} := -(\boldsymbol{M}_x - \boldsymbol{M}_{xn})\ddot{\boldsymbol{x}} - \boldsymbol{C}_x\dot{\boldsymbol{x}} + \boldsymbol{J}^{-\mathrm{T}}\boldsymbol{\tau}_f. \quad (34)$$

$\boldsymbol{f}_{dis} \in \mathbb{R}^3$ of (34) is the disturbance to the desired relationship (31) which consists of the variation of the inertia from the nominal value, the centrifugal and coriolis forces and friction force. From (33), $\boldsymbol{f}_{dis}$ can be calculated with the well known signals as

$$\boldsymbol{f}_{dis} = \boldsymbol{M}_{xn}\ddot{\boldsymbol{x}} + \boldsymbol{D}\dot{\boldsymbol{x}} + \boldsymbol{K}(\boldsymbol{x} - \boldsymbol{x}_{ref}) - \boldsymbol{f}_{ext} + \boldsymbol{f}_{cmp}. \quad (35)$$

The compensator $\boldsymbol{f}_{cmp}$ is given by $\boldsymbol{f}_{dis}$ with a lowpass filter:

$$\boldsymbol{F}_{cmp}(s) = \boldsymbol{G}_{LP}(s)\boldsymbol{F}_{dis}(s), \quad (36)$$

where $\boldsymbol{F}_{cmp}$ and $\boldsymbol{F}_{dis}$ are the Laplace transforms of $\boldsymbol{f}_{ext}$ and $\boldsymbol{f}_{dis}$ and $\boldsymbol{G}_{LP}(s)$ is the transfer function of the lowpass filter. The whole system connected with the disturbance observer

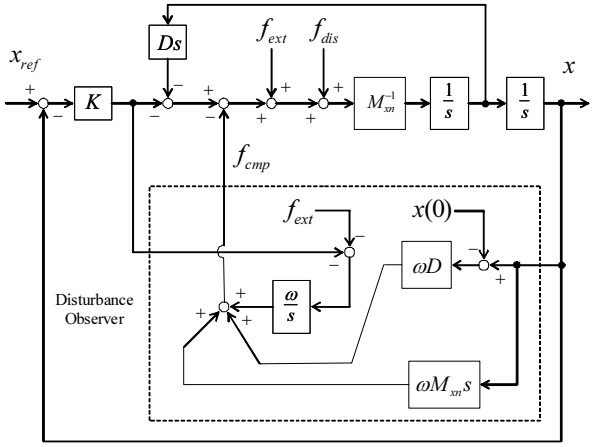

Fig. 5. The block diagram of the whole system with the equivalent disturbance observer.

is illustrated as the block diagram as shown in Fig. 4. From (35), (36) and $\boldsymbol{G}_{LP}(s) = \frac{\omega}{s+\omega}\boldsymbol{I}_3$, $\boldsymbol{F}_{cmp}$ is given by

$$\boldsymbol{F}_{cmp}(s) = \omega \boldsymbol{M}_{xn} s \boldsymbol{X}(s) + \omega \boldsymbol{D}\boldsymbol{X}(s) + \frac{\omega}{s}\left\{\boldsymbol{K}(\boldsymbol{X}(s) - \boldsymbol{X}_{ref}(s)) - \boldsymbol{F}_{ext}(s)\right\}, \quad (37)$$

where $\boldsymbol{X}(s)$ and $\boldsymbol{X}_{ref}(s)$ are the Laplace transforms of $\boldsymbol{x}$and $\boldsymbol{x}_{ref}$. Consequentially, from (37), we get the compensator $\boldsymbol{f}_{cmp}$:

$$\boldsymbol{f}_{cmp} = \omega \boldsymbol{M}_{xn}\dot{\boldsymbol{x}} + \omega \boldsymbol{D}(\boldsymbol{x} - \boldsymbol{x}(0)) + \omega \int \left\{\boldsymbol{K}(\boldsymbol{x} - \boldsymbol{x}_{ref}) - \boldsymbol{f}_{ext}\right\} dt. \quad (38)$$

(38) is the practical compensator whose block diagram is illustrated in Fig. 5. In (38), note that $\boldsymbol{f}_{ext}$ is measured by the force sensor and $(\boldsymbol{x}, \dot{\boldsymbol{x}})$ can be calculated by $(\boldsymbol{q}, \dot{\boldsymbol{q}})$.

B. Stability analysis

We make the following assumption of $\boldsymbol{f}_{ext}$:

Assumption 4: The finger does not slip in the wall. The external force $\boldsymbol{f}_{est}$ is expressed by the linear elastic stiffness given by

$$\boldsymbol{f}_{ext} = \begin{cases} -\boldsymbol{K}_O(\boldsymbol{x} - \boldsymbol{x}_O) & (x \geq x_O) \\ \boldsymbol{0} & (x < x_O) \end{cases} \quad (39)$$
$$\boldsymbol{x}_O := [x_O \ y_O \ z_O]^{\mathrm{T}}, \ \boldsymbol{K}_O \succ 0,$$

where $\boldsymbol{K}_O \in \mathbb{R}^{3\times 3}$ is the stiffness matrix of the wall and $\boldsymbol{x}_O \in \mathbb{R}^3$ is the position of the wall at the contact point.

The following stability theorem holds:

Theorem 2: $\boldsymbol{x}(0) = \boldsymbol{0}$ without loss of generality. Suppose $\boldsymbol{x}_O$ is constant. Define $\alpha > 0$, $0 < \beta < 1$, $0 < \gamma < 2$ and

$$\begin{aligned}
\boldsymbol{S}_1 &:= \bar{\boldsymbol{K}} + \omega \boldsymbol{D} \\
\boldsymbol{S}_2 &:= \alpha\beta \boldsymbol{S}_1 - \omega \bar{\boldsymbol{K}} \\
\boldsymbol{S}_3 &:= (1-\beta)\boldsymbol{S}_1 - \alpha^2 \boldsymbol{M}_x \quad (40) \\
\boldsymbol{T}_1 &:= \alpha \boldsymbol{S}_1 - \omega \bar{\boldsymbol{K}} \\
\boldsymbol{T}_2 &:= \boldsymbol{D} + \omega \boldsymbol{M}_{xn} - \alpha \boldsymbol{M}_x - \tfrac{\alpha^2}{2\gamma}\boldsymbol{T}_3^{\mathrm{T}}\boldsymbol{T}_1^{-1}\boldsymbol{T}_3 \\
\boldsymbol{T}_3 &:= \boldsymbol{D} + \boldsymbol{C}_x + \omega \boldsymbol{M}_{xn} - \dot{\boldsymbol{M}}_x \\
\bar{\boldsymbol{K}} &:= \boldsymbol{K} + \boldsymbol{K}_O. \quad (41)
\end{aligned}$$

Suppose Assumption 4 and that there exist α, β, γ such that

$$\boldsymbol{S}_2, \ \boldsymbol{S}_3, \ \boldsymbol{T}_2 \succ 0. \quad (42)$$

Then, the following and (30) hold:

$$\lim_{t\to\infty} \boldsymbol{x}(t) = \bar{\boldsymbol{x}}_{ref}, \ \lim_{t\to\infty} \dot{\boldsymbol{x}}(t) = \boldsymbol{0}, \quad (43)$$

where

$$\bar{\boldsymbol{x}}_{ref} := \bar{\boldsymbol{K}}^{-1}(\boldsymbol{K}\boldsymbol{x}_{ref} + \boldsymbol{K}_O \boldsymbol{x}_O). \quad (44)$$

Proof: Consider a function as a Lyapunov function given by

$$\begin{aligned}
V(\boldsymbol{x}, \dot{\boldsymbol{x}}, \bar{\boldsymbol{\xi}}) := &\frac{1}{2}\dot{\boldsymbol{x}}^{\mathrm{T}}\boldsymbol{M}_x\dot{\boldsymbol{x}} + \frac{1}{2}(\boldsymbol{x} - \bar{\boldsymbol{x}}_{ref})^{\mathrm{T}}\boldsymbol{S}_1(\boldsymbol{x} - \bar{\boldsymbol{x}}_{ref}) \\
&+ (\boldsymbol{x} - \bar{\boldsymbol{x}}_{ref})^{\mathrm{T}}\omega\bar{\boldsymbol{K}}\bar{\boldsymbol{\xi}} \\
&+ \frac{1}{2}\alpha\bar{\boldsymbol{\xi}}^{\mathrm{T}}\omega\bar{\boldsymbol{K}}\bar{\boldsymbol{\xi}} + \alpha\dot{\boldsymbol{x}}^{\mathrm{T}}\boldsymbol{M}_x(\boldsymbol{x} - \bar{\boldsymbol{x}}_{ref}), \quad (45)
\end{aligned}$$

where

$$\bar{\boldsymbol{\xi}} := \boldsymbol{\xi} + \bar{\boldsymbol{K}}^{-1}\boldsymbol{D}\bar{\boldsymbol{x}}_{ref} \quad (46)$$
$$\boldsymbol{\xi} := \int(\boldsymbol{x} - \bar{\boldsymbol{x}}_{ref})dt \quad (47)$$

From the parameter β and (40), the completing square of (45) is obtained as

$$\begin{aligned}
V = &\frac{1}{2}\beta\boldsymbol{\eta}_1^{\mathrm{T}}\boldsymbol{S}_1\boldsymbol{\eta}_1 + \frac{1}{2}(1-\beta)\boldsymbol{\eta}_2^{\mathrm{T}}\boldsymbol{S}_1\boldsymbol{\eta}_2 + \frac{1}{2}\boldsymbol{\eta}_3^{\mathrm{T}}\boldsymbol{S}_2^{-1}\boldsymbol{\eta}_3 \\
&+ \frac{1}{2}\boldsymbol{\eta}_4^{\mathrm{T}}\boldsymbol{S}_3^{-1}\boldsymbol{\eta}_4, \quad (48)
\end{aligned}$$

where

$$\begin{aligned}
\boldsymbol{\eta}_1 &:= \boldsymbol{x} - \bar{\boldsymbol{x}}_{ref} + \beta^{-1}\boldsymbol{S}_1^{-1}\omega\bar{\boldsymbol{K}}\bar{\boldsymbol{\xi}} \\
\boldsymbol{\eta}_2 &:= \boldsymbol{x} - \bar{\boldsymbol{x}}_{ref} + (1-\beta)^{-1}\boldsymbol{S}_1^{-1}\alpha\boldsymbol{M}_x\dot{\boldsymbol{x}} \\
\boldsymbol{\eta}_3 &:= \sqrt{\alpha}\omega\bar{\boldsymbol{K}}\bar{\boldsymbol{\xi}}, \ \boldsymbol{\eta}_4 := \alpha\boldsymbol{M}_x\dot{\boldsymbol{x}}
\end{aligned}$$

Therefore, $V \succ 0$ from (42).

The differential of V is calculated as

$$\begin{aligned}
\dot{V} = &\dot{\boldsymbol{x}}^{\mathrm{T}}\boldsymbol{M}_x\ddot{\boldsymbol{x}} + \dot{\boldsymbol{x}}^{\mathrm{T}}(\bar{\boldsymbol{K}} + \omega\boldsymbol{D})(\boldsymbol{x} - \bar{\boldsymbol{x}}_{ref}) + \dot{\boldsymbol{x}}^{\mathrm{T}}\omega\bar{\boldsymbol{K}}\bar{\boldsymbol{\xi}} \\
&+ \frac{1}{2}\dot{\boldsymbol{x}}^{\mathrm{T}}\dot{\boldsymbol{M}}_x\dot{\boldsymbol{x}} + (\boldsymbol{x} - \bar{\boldsymbol{x}}_{ref})^{\mathrm{T}}\omega\bar{\boldsymbol{K}}(\boldsymbol{x} - \bar{\boldsymbol{x}}_{ref}) \\
&+ \alpha(\boldsymbol{x} - \bar{\boldsymbol{x}}_{ref})^{\mathrm{T}}\omega\bar{\boldsymbol{K}}\bar{\boldsymbol{\xi}} + \alpha(\boldsymbol{x} - \bar{\boldsymbol{x}}_{ref})^{\mathrm{T}}\boldsymbol{M}_x\ddot{\boldsymbol{x}} \\
&+ \alpha\dot{\boldsymbol{x}}^{\mathrm{T}}\dot{\boldsymbol{M}}_x(\boldsymbol{x} - \bar{\boldsymbol{x}}_{ref}) + \alpha\dot{\boldsymbol{x}}^{\mathrm{T}}\boldsymbol{M}_x\dot{\boldsymbol{x}} + \dot{\boldsymbol{x}}^{\mathrm{T}}\boldsymbol{J}^{\mathrm{T}}\boldsymbol{\tau}_f. \quad (49)
\end{aligned}$$

Here, from (29), (32), (38) and (39), the closed loop system is given by

$$\begin{aligned}
&\boldsymbol{M}_x\ddot{\boldsymbol{x}} + (\boldsymbol{C}_x + \boldsymbol{D} + \omega\boldsymbol{M}_{xn})\dot{\boldsymbol{x}} + \bar{\boldsymbol{K}}(\boldsymbol{x} - \bar{\boldsymbol{x}}_{ref}) \\
&+ \omega\boldsymbol{D}\boldsymbol{x} + \omega\int\bar{\boldsymbol{K}}(\boldsymbol{x} - \bar{\boldsymbol{x}}_{ref})dt = \boldsymbol{J}^{\mathrm{T}}\boldsymbol{\tau}_f. \quad (50)
\end{aligned}$$

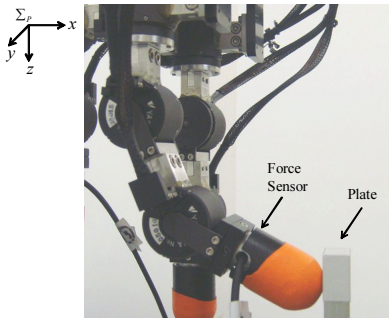

Fig. 6. Experimental setup of the compliance control.

Substituting (50) into (49) and calculating the resultant equation with (28) and the passivity property of the mechanical system $\boldsymbol{M}_x^{\mathrm{T}} = \boldsymbol{M}_x,\ (\dot{\boldsymbol{M}}_x - 2\boldsymbol{C}_x)^{\mathrm{T}} = -(\dot{\boldsymbol{M}}_x - 2\boldsymbol{C}_x)$ leads to

$$\begin{aligned}\dot{V} = &-(\boldsymbol{x} - \bar{\boldsymbol{x}}_{ref})^{\mathrm{T}}\{\alpha(\bar{\boldsymbol{K}} + \omega\boldsymbol{D}) - \omega\bar{\boldsymbol{K}}\}(\boldsymbol{x} - \bar{\boldsymbol{x}}_{ref}) \\ &- \dot{\boldsymbol{x}}^{\mathrm{T}}(\boldsymbol{D} + \omega\boldsymbol{M}_{xn} - \alpha\boldsymbol{M}_x)\dot{\boldsymbol{x}} \\ &- \alpha(\boldsymbol{x} - \bar{\boldsymbol{x}}_{ref})^{\mathrm{T}}(\boldsymbol{D} + \boldsymbol{C}_x + \omega\boldsymbol{M}_{xn} - \dot{\boldsymbol{M}}_x)\dot{\boldsymbol{x}} \\ &+ \dot{\boldsymbol{q}}^{\mathrm{T}}\boldsymbol{\tau}_f. \end{aligned} \tag{51}$$

The completing square of (51) is obtained as

$$\begin{aligned}\dot{V} = &-\frac{1}{2}(2-\gamma)(\boldsymbol{x} - \bar{\boldsymbol{x}}_{ref})^{\mathrm{T}}\boldsymbol{T}_1(\boldsymbol{x} - \bar{\boldsymbol{x}}_{ref}) - \frac{1}{2}\boldsymbol{\eta}_5^{\mathrm{T}}\boldsymbol{T}_1\boldsymbol{\eta}_5 \\ &- \frac{1}{2}\dot{\boldsymbol{x}}^{\mathrm{T}}\boldsymbol{T}_2\dot{\boldsymbol{x}} + \dot{\boldsymbol{q}}^{\mathrm{T}}\boldsymbol{\tau}_f, \end{aligned} \tag{52}$$

where

$$\boldsymbol{\eta}_5 := \sqrt{\gamma}(\boldsymbol{x} - \bar{\boldsymbol{x}}_{ref}) + \tfrac{\alpha}{\sqrt{\gamma}}\boldsymbol{T}_1^{-1}\boldsymbol{T}_3\dot{\boldsymbol{x}}.$$

Note that $\boldsymbol{S}_2 \succ 0 \Rightarrow \boldsymbol{T}_1 \succ 0$ and $\dot{\boldsymbol{q}}^{\mathrm{T}}\boldsymbol{\tau}_f \leq 0$ because $\boldsymbol{\tau}_f$ is the friction and this direction is opposite of $\dot{\boldsymbol{q}}$. From this fact and (42), $\dot{V} \leq 0$ holds.

From LaSalle's invariant principle, V is bounded in the set $X_{\dot{V}=0}$ of $(\bar{\boldsymbol{\xi}}, \boldsymbol{x}, \dot{\boldsymbol{x}})$ with $\dot{V} \leq 0$. Then, the maximum invariant set to satisfy $\dot{V} \equiv 0$ is given by $(\bar{\boldsymbol{\xi}}, \boldsymbol{x}, \dot{\boldsymbol{x}}) = (\bar{\boldsymbol{K}}^{-1}\boldsymbol{D}\bar{\boldsymbol{x}}_{ref}, \bar{\boldsymbol{x}}_{ref}, \boldsymbol{0})$. Therefore, the trajectory of the solution of (50) with the start point in $X_{\dot{V}=0}$ converges to $(\bar{\boldsymbol{\xi}}, \boldsymbol{x}, \dot{\boldsymbol{x}}) = (\bar{\boldsymbol{K}}^{-1}\boldsymbol{D}\bar{\boldsymbol{x}}_{ref}, \bar{\boldsymbol{x}}_{ref}, \boldsymbol{0})$.

Finally, we prove (30). From (39) and (44), both the sides of (30) are calculated as

$$\begin{aligned}\boldsymbol{K}(\boldsymbol{x} - \boldsymbol{x}_{ref}) &= \boldsymbol{K}\bar{\boldsymbol{K}}^{-1}\boldsymbol{K}_O(\boldsymbol{x}_O - \boldsymbol{x}_{ref}) \\ \boldsymbol{f}_{ext} &= \boldsymbol{K}_O\bar{\boldsymbol{K}}^{-1}\boldsymbol{K}(\boldsymbol{x}_O - \boldsymbol{x}_{ref}).\end{aligned}$$

Note that the following relationship of $\bar{\boldsymbol{K}}$ holds:

$$\begin{aligned}\boldsymbol{K}^{-1}(\boldsymbol{K} + \boldsymbol{K}_O)\boldsymbol{K}_O^{-1} &= \boldsymbol{K}_O^{-1}(\boldsymbol{K} + \boldsymbol{K}_O)\boldsymbol{K}^{-1} \\ \Leftrightarrow \boldsymbol{K}_O\bar{\boldsymbol{K}}^{-1}\boldsymbol{K} &= \boldsymbol{K}\bar{\boldsymbol{K}}^{-1}\boldsymbol{K}_O.\end{aligned}$$

Therefore, (30) is proved. ∎

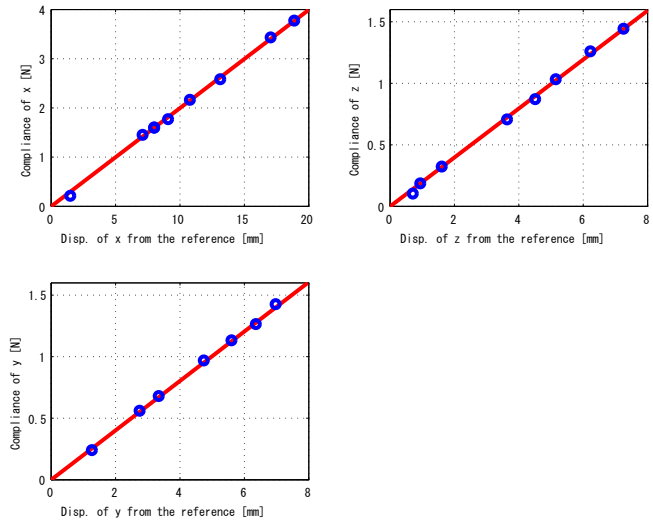

Fig. 7. Verification of the compliance.

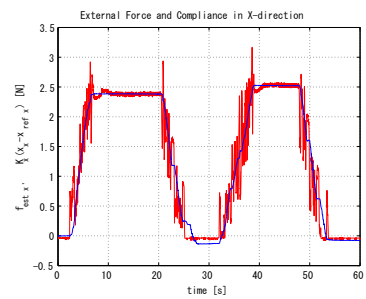

Fig. 8. Compliance control with the varying x_{ref} in x direction.

IV. Experiments

A. Verification of the compliance controller

The performance of the compliance controller is verified. The equilibrium is set to $q_1 = 0$ and $q_2 = q_3 = 30$ [deg] and the control parameters are set to

$$\begin{aligned}\boldsymbol{K} &= \text{block diag}(200, 200, 200)[\mathrm{N/m}] \\ \boldsymbol{D} &= \text{block diag}(45, 45, 45)[\mathrm{Ns/m}] \\ \omega &= 30[\mathrm{rad/s}].\end{aligned} \tag{53}$$

The displacement of the finger is produced by pushing the plate attached to the XY-table as shown inFig. 6. The finger position is calculated by the joint angles and the external force is measured by the force sensor attached to the center of the finger-tip. The sampling time of the control is 1[ms].

First, verify the static relationship. After setting the displacement of the finger, the average values of the 100 sampled data of the forces in the x, y and z-axes are shown in Fig. 7. The blue and red lines represents the average values and the approximated line with the least-squares method. It is confirmed that the static compliance is achieved because the coefficients of the red lines in (x, y, z) are $199.75[\mathrm{N/m}]$, $200.87[\mathrm{N/m}]$ and $198.97[\mathrm{N/m}]$.

In the grasp with the controller, the $\boldsymbol{x}_O$ is *time varying*. This case is however not proved in the previous section.

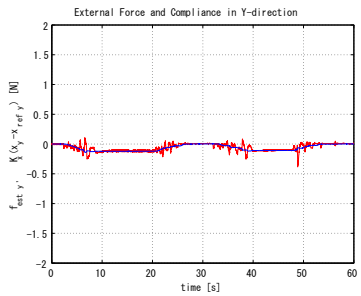

Fig. 9. Compliance control with the varying x_{ref} in y direction.

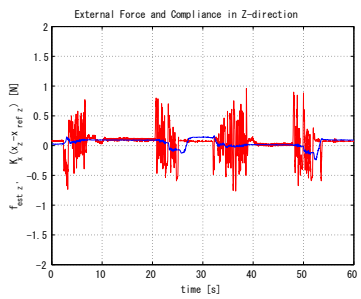

Fig. 10. Compliance control with the varying x_{ref} in z direction.

Therefore, second, verify the dynamic performance *experimentally* when $\boldsymbol{x}_O$ is time varying. The result is shown in Figs. 8–10, where the plate is moved with time varying displacement. The blue lines represent the compliance $\boldsymbol{K}(\boldsymbol{x}-\boldsymbol{x}_{ref})$ and the red lines represents the external force. It is confirmed that the compliances are close to the time varying external force with a little oscillation in the x and y directions. The external force in the z direction changes with big amplitudes because the finger-tip is a semi-sphere and it is not considered in the controller.

B. Verification of stable grasp

Here, the stability of the grasp with the sufficient condition derived in Section 2 is verified by the compliance controller. The object is a circular cylinder with the height127[mm], the radius 75[mm] and the mass 132[g] as shown in Fig. 11 (a). The contact points are located at the edge of the circle from the upper edge of the object with 30[mm]. The angles of the contact points are set to 30, -30 and 180 [deg] from the x-axis. Figure 11 (b) shows the frames Σ_{S_i} and Σ_B. Σ_B is fixed to the center of the circle. The control parameters are set to the same ones of (53) in the cases of the 1st and 2nd fingers and $\boldsymbol{K}$ = block diag$(200\sqrt{3}, 200\sqrt{3}, 200\sqrt{3})$[N/m] in the case of the 3rd finger. Note that these are expressed in the spring frame Σ_{S_i}. The initial spring displacements δ_{0x_i} are set to $(2.5, 2.5, 2.5\sqrt{3})$[N] in the $-x$-axis and δ_{0z_i} is set to the values to balance the gravity. The disturbance is generated by a human hand with slow movement as shown in Fig. 13. To verify whether the position and orientation of the object are recovered to the initial state, the position and orientation are measured by the 2-eyes cameras with the white markers as in Fig. 12. It is confirmed that the object

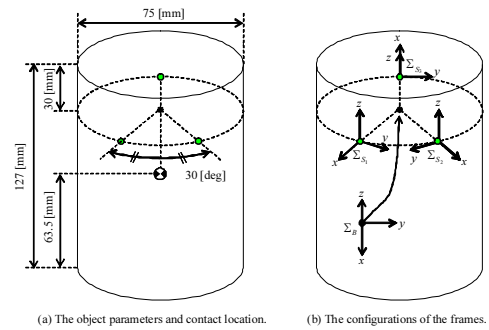

(a) The object parameters and contact location. (b) The configurations of the frames.

Fig. 11. A cylinder object in the stable grasping

is recovered to the initial state by the measurements using the eye.

The time response of the object is shown in Fig. 15. The left and right columns represent the position and orientation. It is confirmed that the very lines are recovered to the initial states though they are perturbed by the disturbance.

V. Conclusions

In this paper, we dealt with an analysis and a synthesis of stable grasp by a multi-fingered robot hand with compliance control. The stability of a grasped object by the fingers with linear elastic stiffness was firstly analyzed. A sufficient condition with the gravity effect was driven with respect to the contact points, the elastic coefficients and the mass of the grasped object. A compliance controller with a disturbance observer using force sensors secondly was secondly proposed. The stability of the controller was proved by the Lyapunov stability theorem with a sufficient condition. The performance of the controller was verified in experiments. Furthermore, it was verified that the grasp by the compliance controller was stable with the sufficient condition.

Future works are mentioned here. The center of gravity of the object for stable grasp is restricted under the contact points. This is a little trivia because of the analogy of the stability of a pendulum. The grasp with the virtual springs is expected to stabilize the object when the contact points are located above the center of gravity. This is an important challenge for us. The performance of the compliance control in the z-direction deteriorated because the finger-tip rolled on the plate. It is ncecessary to consider the contact movement due to the shape of the finger-tip. The gear ratios of the motors of the fingers are large for enough torque because the power of the motor is small due to its miniaturization. Therefore, the effect of the joint friction is larger than the effect of the inertia and gravity. It is important to analyze the control performance with respect to the disturbance due to the friction. The stability of disturbance controller was proved in only the case of constant $\boldsymbol{x}_O$ and the its performance in the case of time varying $\boldsymbol{x}_O$ was confirmed only experimentally. It is necessary to prove the stability in the case of time varying $\boldsymbol{x}_O$ for the grasp with the compliance controller.

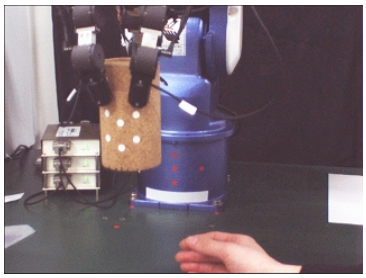

Fig. 12. Grasp without disturbance

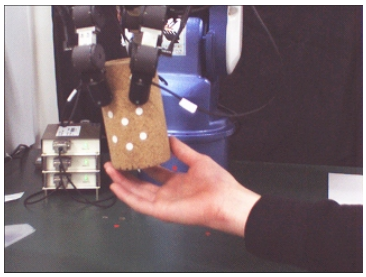

Fig. 13. Grasp with disturbance

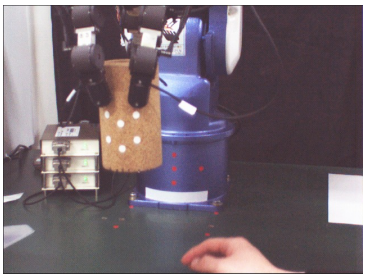

Fig. 14. Grasp after disturbance

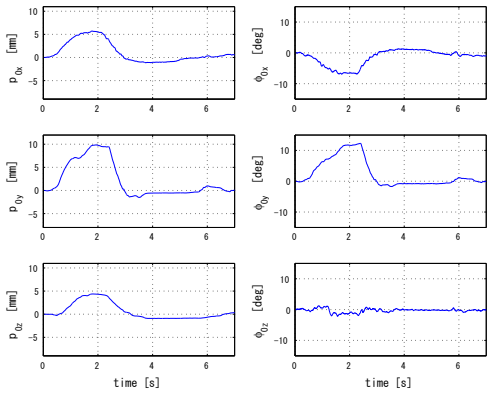

Fig. 15. Position and orientation of the grasped object when it is disturbed.

REFERENCES

[1] V. Nguyen: Constructing Force-Closure Grasps, *Int. J. Robot. Res.*, Vol. 7, No. 3, pp. 3–16, 1988.

[2] J. Kerr and B. Roth: Analysis of Multifingered Hands, *Int. J. Robot. Res.*, Vol. 4, No. 4, pp. 3–17, 1986.

[3] Y. Nakamura, K. Nagai and T. Yoshikawa: Dynamics and Stability in Coordination of Multiple Robotic Mechanisms, *Int. J. Robot. Res.*, Vol. 8, No. 2, pp. 44–61, 1989.

[4] T. Yoshikawa and K. Nagai: Manipulating and Grasping Forces in Manipulation by Multifingered Robot Hands, *IEEE Trans. Robot. Automat.*, Vol. 7, No. 1, pp. 67–77, 1991.

[5] T. Watanabe and T. Yoshikawa: Optimization of Grasping an Object by Using Required Acceleration and Equilibrium-Force Sets, *Proc. IEEE/ASME Int. Conf. on Advanced Intel. Mech.*, pp. 338–343, 2003.

[6] M. Cutkosky and I. Kao: Computing and Controlling the Compliance of a Robot Hand, *IEEE Trans. Robot. Automat.*, Vol. 5, No. 2, pp. 151–165, 1989.

[7] H. Hanafusa and H. Asada: Stable Prehension by a Robot Hand with Elastic Fingers, *Pric. 7th Int. Symp. on Industrial Robots*, pp. 361–368.

[8] M. Kaneko, N. Imamura, K. Yokoi and K. Tanie, A Realization of Stable Grasp Based on Virtual Stiffness Model by Robot Fingers, IEEE Int. Workshop on Advanced Motion Control, pp.156–163, 1990.

[9] T. Yamada, T. Kuraishi, Y. Mizuno, N. Mimura and Y. Funahashi: Stability Analysis of 3D Grasps by A Multifingered Hand, *Proc. IEEE Int. Conf. on Robot. Auto.*, pp. 2566–2473 2001.

[10] C. Ott, A. Albu, A. Kugi and G. Hirzinger: On the Passivity-Based Inmpedance control of Flexible Joint Robots, *IEEE Trans. Robot.*, Vol. 24, No. 2, pp. 416–429, 2008.

[11] Z. Doulgeri and S. Arimoto: A Force Commanded Impedance Control for a Robot Finger with Uncertain Kinematics, *Int. J. Robot. Res.*, Vol. 18, No. 10, pp. 1013–1029, 1999.

[12] S. Chen, K. K. Tan and S. Huang: Friction Modeling and Compensation of Servomechanical Systems with Dual-Relay Feedback Approach, *IEEE Trans. Cont. Sys. Tech.*, Vol. 17, No. 6, pp. 1295–1305, 2009.

[13] K. Ohnishi, M. Shibata and T. Murakami: Motion Control for Advanced Mechatronics, *IEEE/ASME Trans. on Mech*, Vol. 1, No. 1, pp. 56–67 1996.

[14] S. Komada, M. Ishida, K. Ohnishi and T. Hori: Disturbance observer-based motion control of direct drive motors, *IEEE Trans. Ener. Conv.*, Vol. 6, No. 3, pp. 553—559, 1991.

[15] T. Murakami, N. Oda, Y. Miyasaka and K. Ohnishi: A motion control strategy based on equivalent mass matrix in multidegree-of-freedom manipulator, *IEEE Trans. Ind. Electr.*, Vol. 42, No. 2, pp. 123–130, 1995.

[16] S. Komada and K. Ohnishi: Force feedback control of robot manipulator by the acceleration tracing orientation method, *IEEE Trans. Ind. Electr.*, Vol. 37, No. 1, pp. 6–12, 1990.

[17] S. Katsura, Y. Matsumoto and K. Ohnishi: Analysis and experimental validation of force bandwidth for force control, *IEEE Trans. Ind. Electr.*, Vol. 53, No. 3, pp. 922–928, 2006.

[18] T. Murakami, N. Oda, Y. Miyasaka and K. Ohnishi: Force sensorless impedance control by disturbance observer, *Proc. of Power conv. Conf.*, pp. 352–357, 1993.

[19] R. Bichel and M. Tomizuka: Hybrid Impedance Control in Constraint Coordinates Using a Disturbance Observer, *Proc. of CDC*, pp. 1974–1979, 1996.

[20] K. Kaneko, K. Ohnishi and K. Komoriyama: A design method for manipulator control based on disturbance observer, *Proc. of IROS*, pp. 1405–1412, 1994.

[21] H. Kobayashi, S. Katsura and K. Ohnishi: An Analysis of Parameter Variations of Disturbance Observer for Motion Control, *IEEE Trans. Ind. Electr.*, Vol. 54, No. 6, pp. 3413–3421, 2007.